Journal of
Materials Chemistry A

COMMUNICATION

Supporting Information

Redox Inactive Ions Meliorated $BaCo_{0.4}Fe_{0.4}Zr_{0.1}Y_{0.1}O_{3-\delta}$ Perovskite Oxides as Efficient Electrocatalysts for Oxygen Evolution Reaction

Xiangnan Li [a,d†], Jie Zhang[a†], Qi Feng[a], Chunying Pu[b], Luozheng Zhang[a], Manman Hu[a], Xianyong Zhou[a], Xiongwei Zhong[a], Wendi Yi[a], Jun Tang[a], Zhiwei Li[c], Xingzhong Zhao[d], Hui Li[a], Baomin Xu[a]*

[a]Department of Materials Science and Engineering, Southern University of Science and Technology, Shenzhen, Guangdong Province 518055, China
[b]College of Physics and Electronic Engineering, Nanyang Normal University, Nanyang, Henan Province 473061, China
[c]School of Physical Science and Technology, Lanzhou University, Lanzhou, Gansu Province 730000, China
[d]Deptment of Physics, Wuhan University, Wuhan, Hubei Province 430072, China
† These authors contributed equally.

* Corresponding author, E-mail: xubm@sustc.edu.cn (Baomin Xu)

Experimental Section

Catalysts synthesis: $BaCo_{0.5-x}Fe_{0.5-x}Zr_xY_xO_{3-\delta}$ ($BCF(ZY)_x$, x = 0.05-0.10) and $Ba_{0.5}Sr_{0.5}Co_{0.8}Fe_{0.2}O_{3-\delta}$ (BSCF) oxides were synthesized by a combined EDTA-citrate complexing sol-gel method. Here taking $BCF(ZY)_{0.1}$ as an example, stoichiometric amounts of barium nitrate (Aladdin, ≥99.0%), cobalt (Ⅱ) nitrate (Aladdin, ≥99.0%), iron (Ⅲ) nitrate (Aladdin, ≥98.0%), zirconium (Ⅳ) nitrate (Aladdin, ≥99.0%) and yttrium (Ⅲ) nitrate (Aladdin, ≥99.0%) were weighed, dissolved in deionized water and then added into EDTA-$NH_3 \cdot H_2O$ solution (pH≈9) with stirring to form an aqueous solution. Then citric acid-$NH_3 \cdot H_2O$ solution (pH≈9) was introduced, with the molar ratio of 1:1:2 for EDTA acid: total metal ions: citric acid. The mixed solution was heated at 80 ^oC and 150 ^oC in sequence to obtain a dark dry foam-structure precursor. The precursor was decomposed in a muffle furnace, followed by calcinations at 600 ^oC for 5 h and 1050 ^oC for 10 h in air to yield the desired powders. The commercial catalyst of IrO_2 was purchased from SangLaiTe for comparison.

Physicochemical characterization: The crystal structure of as-synthesized $BaCo_{0.5-x}Fe_{0.5-x}Zr_xY_xO_{3-\delta}$ ($BCF(ZY)_x$, x = 0.05-0.10) powders was characterized by X-ray diffraction measurement (XRD, D/MAX-2400 Rigaku, TOKYO) at room temperature with step size of 0.02^o in 2θ over the scanning angular range of 20^o-80^o. To get more accurate details of crystal structures, zeropoint correction of XRD patterns was carried out based on the X-ray diffraction theory. Then, Rietveld method was used for structure refinement employing the Materials Studio program of reflex plus modules. The morphologies of the catalysts were observed using a field-emission scanning electron microscope (SEM, TESCAN MIRA3). To better observe the particle size and micro-structure, certain amount of catalysts were dispersed into tetrahydrofuran solution by supersonic and then dripped on the clean Cu foil under a reductive heat treatment. The catalysts morphology and structure were further analyzed by

transmission electron microscopy (TEM, Tecnai F30). The cross-sectional TEM samples of catalyst particles were thinned initially by a typical focused ion beam (FIB, FEI Helios 600i) technique and were additionally treated by a low-energy Ar-ion milling system to remove the amorphous layer. To minimize the surface contamination from other foreign impurities and avoid the Ga ion beam damage during the FIB process, the surface of the particles was first coated with sputtered carbon before FIB. The specific surface areas of the catalysts were estimated via Brunauer Emmet Teller (BET, Tristar II plus, Micromeritics) method under nitrogen atmosphere using physisorption analyzer. Oxygen content of the as-synthesized $BCF(ZY)_{0.1}$ sample was determined by iodometric titrations at room temperature with seven parallel analyses to reduce the measurement error. The chemical compositions and surface element sates were determined by X-ray photoelectron spectroscopy (PHI 5000 VersaProbe II). Mössbauer spectroscopy of the $BCF(ZY)_{0.1}$ was recorded using a conventional constant acceleration spectrometer (Wissel, Germany) with a γ-ray source of 25 mCi^{57}Co in a palladium matrix moving at room temperature. The absorber was kept static in a temperature-controllable cryostat. All isomer shifts were quoted relative to α-Fe at room temperature. The oxygen desorption properties were evaluated using oxygen temperature programmed desorption (O_2-TPD, Auto Chem II 2920, Micromeritics). Approximately 0.2 g of each sample was heated in a U-type quartz tube to 250 ^oC with a heating rate of 10 ^oC min^{-1} under pure Ar, and kept at this temperature for 2h. After cooling the sample to room temperature, adsorption of O_2 was carried out in flowing O_2 for 1 hour. For comparison, corresponding blank test without adsorption of O_2 was conducted under the same test process. The gas was then switched to pure Ar until the baseline was stable. After these processes finished, the O_2-TPD measurement was performed up to 700 ^oC with a ramp of 10 ^oC min^{-1} in flowing pure Ar (15 ml min^{-1}). The outlet gases were analyzed by a mass spectrometer to monitor the oxygen concentrations.

Electrochemical measurement: The electrochemical activity of the investigated catalyst was evaluated by using the typical thin film rotating disk electrode (TFRDE) method, which involved the preparation of the catalyst ink, the formation of the thin film of catalyst on the RDE, and the electrochemical measurements carried out in a typical three-electrode electrochemical cell connected to an electrochemical workstation.

Preparation of the catalyst ink: Briefly, the catalyst ink was prepared by sonicating a mixture of 5.0 mg of the catalyst, 1.0 mg of acetylene black (AB) carbon, and 33 μL of K^+ exchanged Nafion solution in the solvent containing 500 μL 2-methoxyl ethanol and 467 μL tetrahydrofuran for 1 h. The AB carbon was treated in nitric acid overnight at 80 ℃, and K^+ exchanged Nafion solution was a mixture of 2/1 volume ratio of Nafion solution (5 wt%) and 0.1 M KOH.

Preparing thin film of the catalyst on the RDE: 10 μL of the catalyst ink was dropped on the glassy carbon RDE (0.196 cm^2 area) polished by 50 nm alumina slurry and rinsed by sonicating in pure water. Then the RDE was rotated at 700 rpm until the film was dry (about 30 min), yielding a catalyst mass loading of 0.255 mg_{oxide} cm_{disk}^{-2}. $BCF(ZY)_{x,}$ BSCF and IrO_2 have the same mass loading in the TFRDE.

Electrochemical systems: Electrochemical measurements were conducted in a typical three-electrode electrochemical cell connected to an electrochemical workstation (CHI 760) and a RDE system (Pine instrument company, USA) at room temperature. A graphite rod electrode was used as the counter electrode. The reference electrode was a Hg|HgO (0.1 M KOH) electrode, which was calibrated with respect to a reversible hydrogen electrode in 0.1 M KOH. The electrolyte was 0.1 M KOH aqueous solution (Acros, 99.98%), which was O_2-saturated by bubbling O_2 into it for more than 30 min prior to test and maintained under O_2 atmosphere throughout.

Measurement procedure: Before all the measurements, the catalyst was electrochemically activated via cyclic voltammetry in the potential range of 0.23 to 0.9 V (versus Hg|HgO) at 100 mV s^{-1} for 40 cycles with a rotating rate of 1600 rpm. The cyclic voltammetry measurement of OER activity was performed at 10 mV s^{-1} and 1600 rpm. The CV curve was capacity corrected by averaging the forward and reverse currents, and ohmic resistance corrected according to the Equation: $E_{iR\text{-}corrected} = E - iR$, where i is the current, and R is the ohmic resistance (~45 Ω) from electrolyte measured via electrochemical impedance spectroscopy. The chronopotentiometry was carried out at 10 mA cm_{disk}^{-2} and 1600 rpm for 2h. Electrochemical impedance spectroscopy measurement was performed at 0.68 V vs Hg|HgO between 10 KHz to 100 mHz with an amplitude of 10 mV.

An anion exchange membrane (AEM) water electrolysis cell preparation: Membrane electrode assemblies (MEAs) were prepared by using the catalysts coated on substrate (CCS) method, as follows. Pt/C (40 wt%, Johnson matthey, HiSPECTM 4000) was used as hydrogen evolution reaction (HER) electrocatalyst for the cathode, and $BCF(ZY)_{0.1}$ was used as oxygen evolution reaction (OER) electrocatalyst for the anode. A201 membrane (Tokuyama Corporation, Japan) with a thickness of 28 μm was used as anion exchange membrane (AEM). The catalyst layer was prepared from a homogenous ink comprising catalyst, isopropyl alcohol, and alkaline ionomer (xQAPS, 2 wt%, WHU) solution. The electrocatalysts loading were 6.37 mg cm^{-2} $BCF(ZY)_{0.1}$ and 1.5 mg cm^{-2} Pt, respectively. The ionomer content in the catalyst layer was approximately 15% for the hydrogen side and the oxygen side. The electrode catalyst ink was sprayed onto microporous carbon paper (TGPH-90, Toray Inc., Japan) using an air spray gun (Iwata, Japan). Both the gas diffusion electrodes (GDEs) were dried at 40 °C for 12 h. The membrane was sandwiched between the anode and cathode GDEs. The MEA was housed between two titanium bipolar plates with flow channels. The entire cell was mechanically tightened to achieve intimate contact between the MEA components. The effective area of the MEA was 2.25 cm^2. A preheated 0.1 M KOH solution

was used as electrolyte for water electrolysis. The electrolyte fed in 30 ml min^{-1} to the anode of the cells and was circulated, from a reservoir, through the anode side by a peristaltic pump. Experiments were carried out at 50 °C.

Computational section: The underlying ab initio structure relaxations were performed in the framework of density functional theory within the generalized gradient approximation[1] as implemented in the VASP code.[2, 3] The electron−ion interaction is described by pseudopotentials built within the projector augmented wave approximation with $2s^2 2p^4$, $3d^7 4s^1$, $3d^8 4s^1$, $4s^2 4p^6 5s^2 4d^1$, $4s^2 4p^6 5s^2 4d^2$ and $5s^2 5p^6 6s^2$ valence electrons for O, Fe, Co, Y, Zr and Ba atoms, respectively.[3, 4] The energy cut-off 400 eV and appropriate Monkhorst-Pack k-meshs with grid spacing of $2\pi \times 0.03$ $Å^{-1}$ in 100 atoms lattice are found to provide sufficient precision in calculating total energy and force for the exchange correlation formalisms. This usually gives total energies well converged within ~1× 10-6 eV/atom. The formation energy of $V_O^{\cdot\cdot}$ in Ba20Co8Fe8Zr2Y2O60 is calculated by the following Equation:[5]

$$\Delta E_{f,vac} = E_{defective\,(V_O^{\cdot\cdot})} + \frac{1}{2}E_{O_2} - E_{perfect}$$

Where $E_{defective\,(V_O^{\cdot\cdot})}$, $E_{perfect}$, and E_{O_2} are the calculated total energy of $V_O^{\cdot\cdot}$ -containing Ba20Co8Fe8Zr2Y2O60, perfect lattice structure Ba20Co8Fe8Zr2Y2O60, and the chemical potential of an O2 molecule. In this work, we use a large 100-atom cell with a quasirandom distribution of Fe/Co/Zr/Y cations on B site.

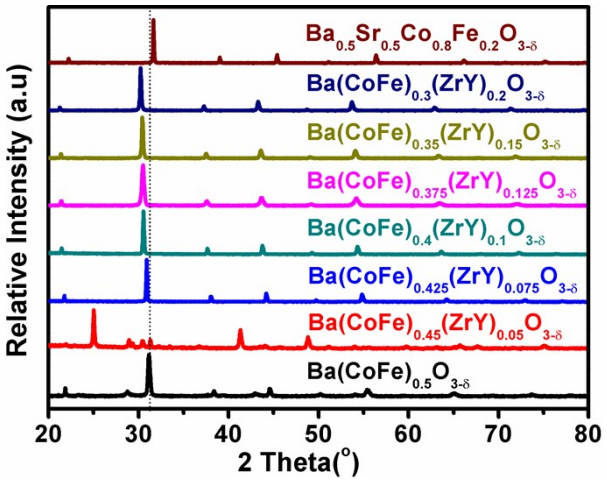

Figure S1. XRD pattern of as-synthesized $BaCo_{0.5-x}Fe_{0.5-x}Zr_xY_xO_{3-\delta}$ (x = 0-0.2) and $Ba_{0.5}Sr_{0.5}Co_{0.8}Fe_{0.2}O_{3-\delta}$ (BSCF).

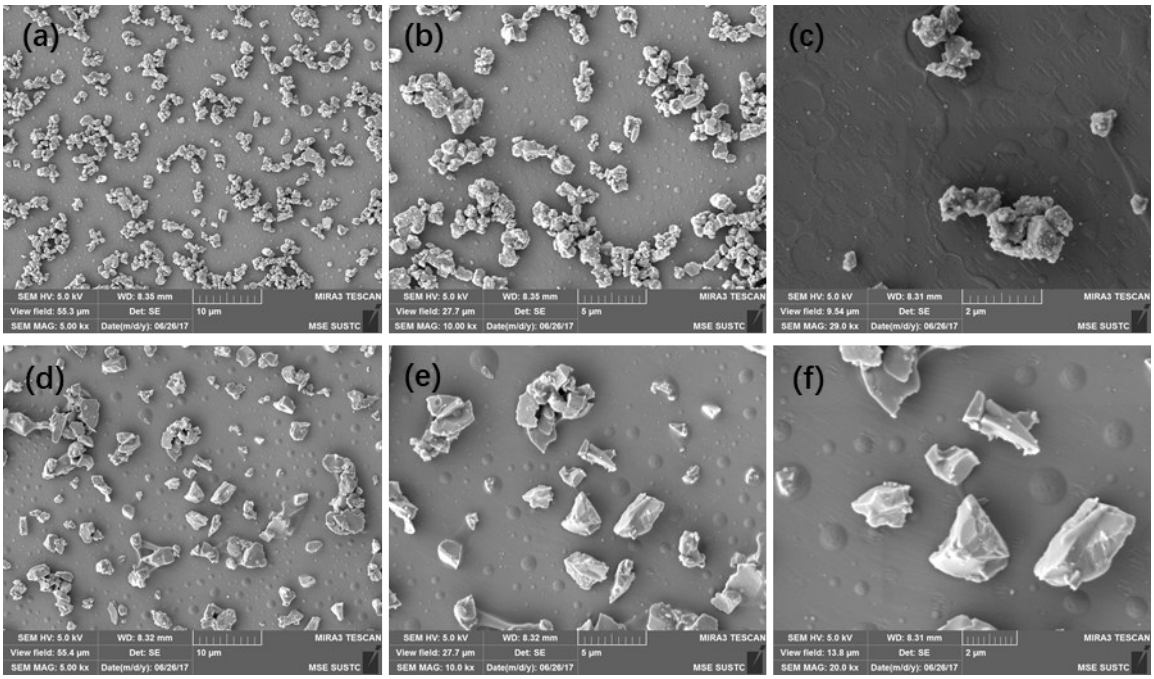

Figure S2. SEM images of as-synthesized $BCF(ZY)_{0.1}$ (a-c) and BSCF(d-f) powders at various resolutions.

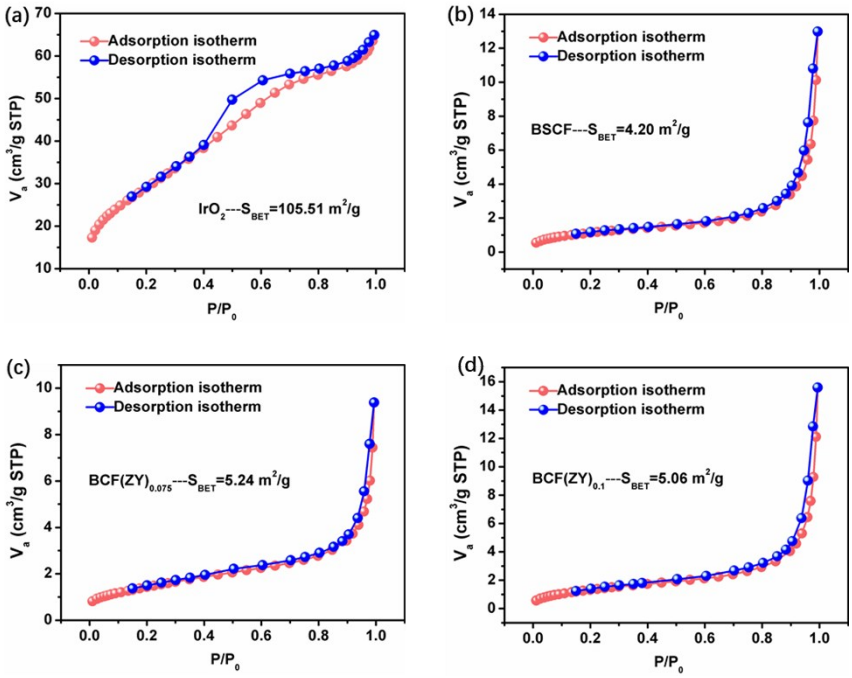

Figure S3. N_2 adsorption-desorption isotherm curve of IrO_2 (a), BSCF (b), $BCF(ZY)_{0.075}$ (c) and $BCF(ZY)_{0.1}$.

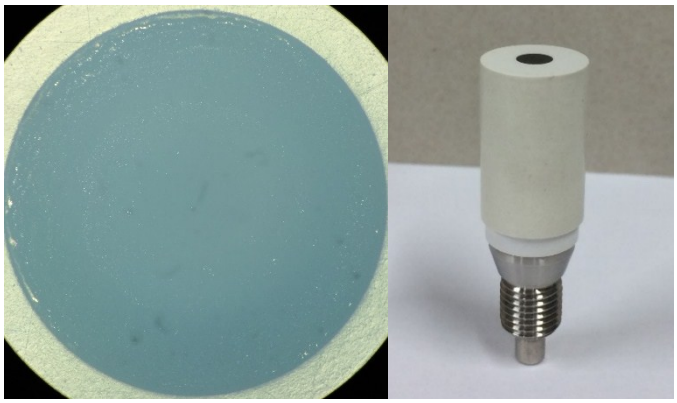

Figure S4. Observed film feature on RDE by using a microscopy.

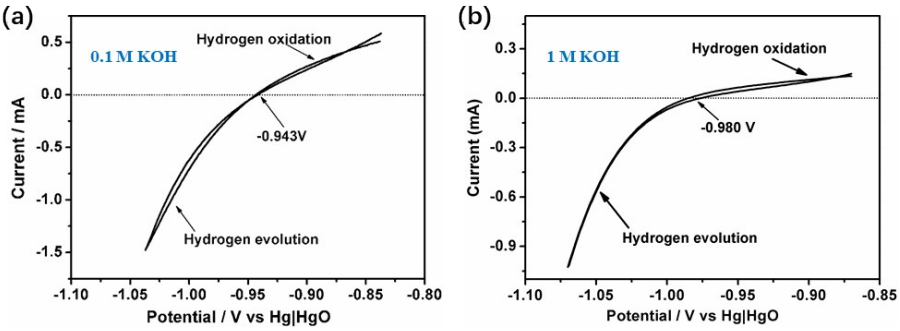

Figure S5. CV curve of Pt mesh working electrode at a scan rate of 1 mV s^{-1} in the ultrahigh purity H_2 -saturated (a) 0.1 M KOH and (b) 1 M KOH solution for RHE calibration of the Hg|HgO electrode (Calibrate the RE with RHE).

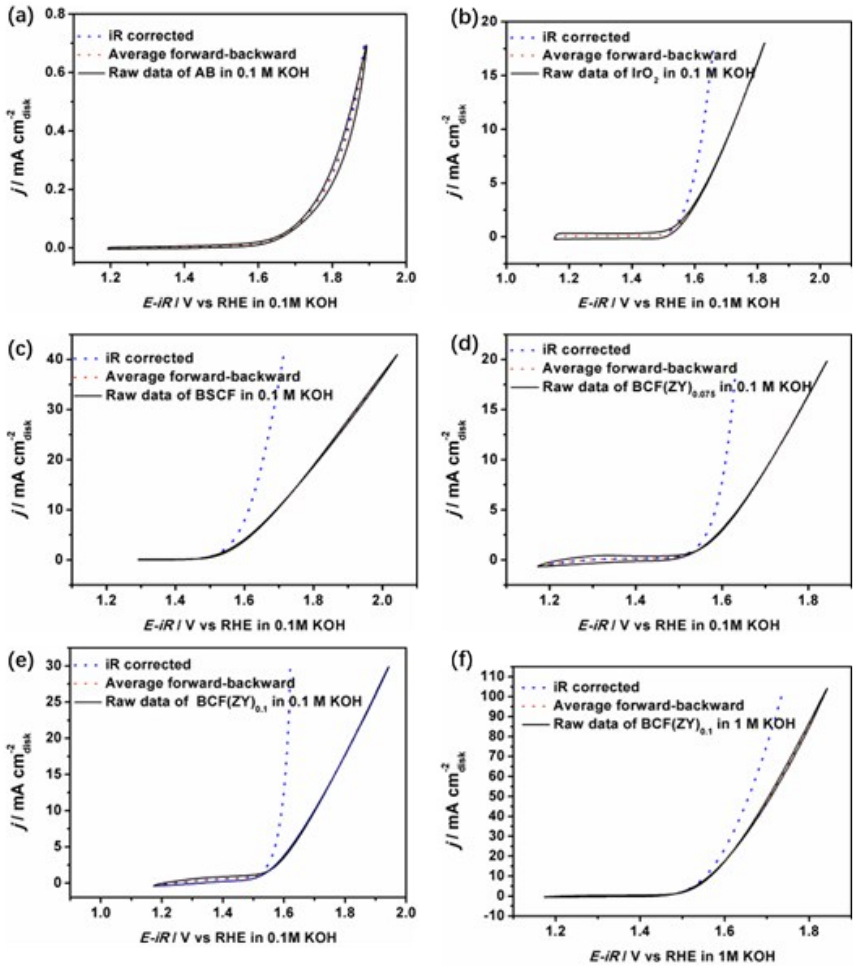

Figure S6. Comparison between CVs with and without iR and capacity correction (Capacitive and ohmic corrections of the as-measured CV curve (10 mV s^{-1}) of conductive acetylene black (AB) (a), IrO_2 (b), BSCF (c), $BCF(ZY)_{0.075}$ (d) and $BCF(ZY)_{0.1}$ (e-f).

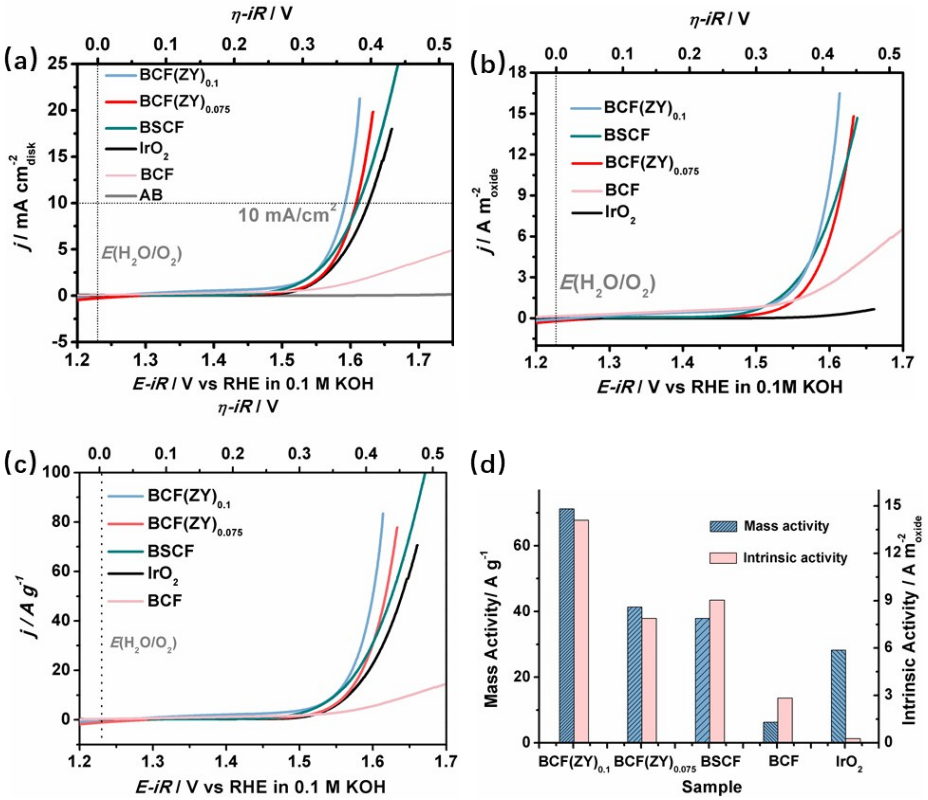

Fig S7. (a) Ohmic and capacitive corrected voltammograms of $Ba(CoFe)_{0.5}O_{3-\delta}$ (BCF), $Ba(CoFe)_{0.425}(ZrY)_{0.075}O_{3-\delta}$ ($BCF(ZY)_{0.075}$), $Ba(CoFe)_{0.4}(ZrY)_{0.1}O_{3-\delta}$ ($BCF(ZY)_{0.1}$), $Ba_{0.5}Sr_{0.5}Co_{0.8}Fe_{0.2}O_{3-\delta}$ (BSCF) and IrO_2 at 10 mV cm^{-2} and 1600 rpm. The background OER activity of a thin-film Nafion-bonded acetylene black (AB) thin film electrode is shown for reference. These curves are averaged from three independent measurements. (b) Mass activity curves of BCF, $BCF(ZY)_{0.075}$, $BCF(ZY)_{0.1}$, BSCF and IrO_2, the current is normalized by the oxides mass loading. (c) Intrinsic OER activity curves of BCF, $BCF(ZY)_{0.075}$, $BCF(ZY)_{0.1}$, BSCF and IrO_2, the current is normalized by the BET surface area of the oxides. (d) The comparison of intrinsic OER activity and mass activity of BCF, $BCF(ZY)_{0.075}$, $BCF(ZY)_{0.1}$, BSCF and IrO_2, catalysts at an overpotential of η=0.38V in 0.1 M KOH.

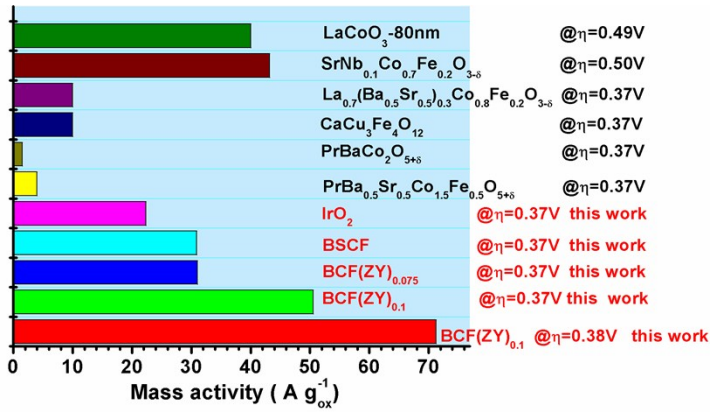

Figure S8. The comparison of mass OER activity of $BCF(ZY)_{0.1}$ with recently reported advanced representative active OER electrocatalysts and IrO_2 suppored on glass catbron electrode (GCE) in alkaline solutions.

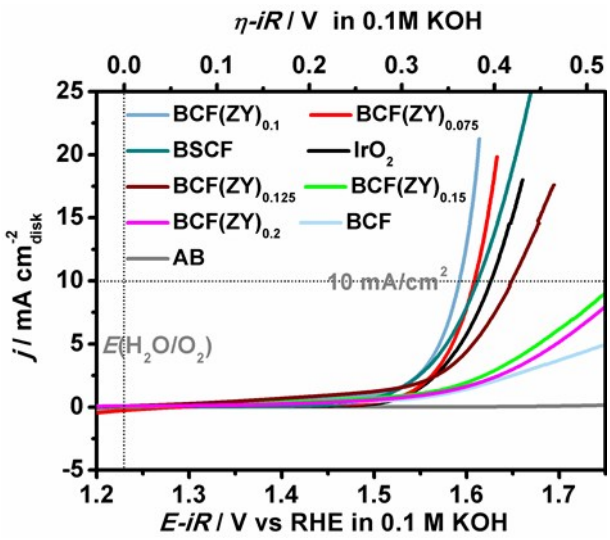

Figure S9.. Ohmic and capacitive corrected voltammograms of $BaCo_{0.5-x}Fe_{0.5-x}Zr_xY_xO_{3-\delta}$ (x = 0-0.2) , $Ba_{0.5}Sr_{0.5}Co_{0.8}Fe_{0.2}O_{3-\delta}$ (BSCF), and IrO_2 at 10 mV cm^{-2} and 1600 rpm.

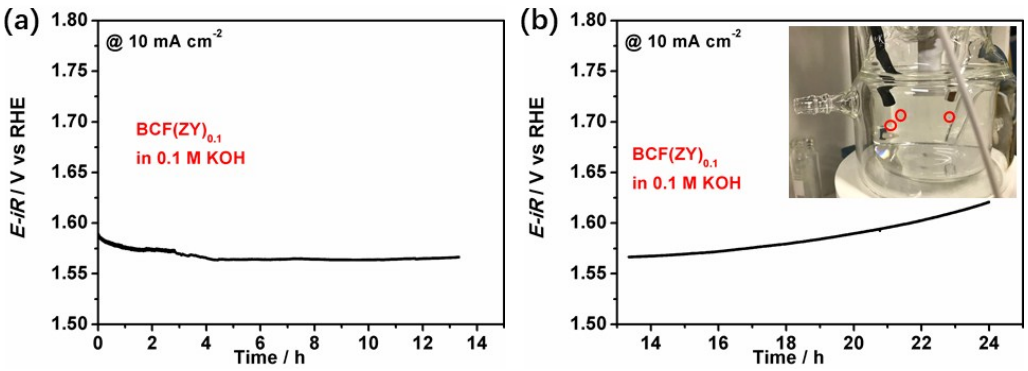

Figure S10. Chronopotentiometry (CP) measurement of the $BCF(ZY)_{0.1}$ catalysts on the RDE at a constant current density of 10 mA cm_{disk}^{-2} in O_2-saturated 0.1 M KOH.

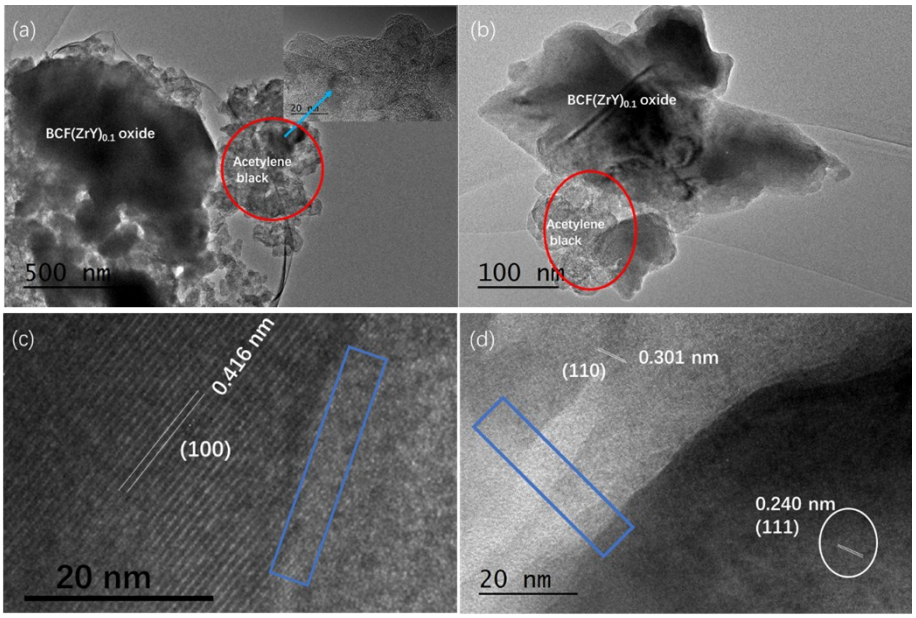

Figure S11. TEM (a-b) and HRTEM (c-d) images of $BCF(ZY)_{0.1}$ catalysts after Chronopotentiometry (CP) measurement for 24 h.

Table S1. Crystalline interplanar spacing of $BCF(ZY)_{0.1}$ oxide before (from XRD) and after (from TEM) CP test for 24 h

	Before CP test (from XRD)	After CP test (from TEM)
(100)	0.411	0.416
(110)	0.291	0.301
(111)	0.237	0.240

Table S2. Comparison of OER activity of $BCF(ZY)_{0.1}$ with recently reported advanced representative active OER electrocatalysts suppored on glass catbron electrode (GCE) in alkaline solutions.

Name	Electrolyte	Mass loading mg_{oxide}/cm^2_{disk}	Tafel slope (mV/dec) (disk)	potential at 10 mA/cm^2	Overpotential at 10 mA $/cm^2$	reference
$BCF(ZY)_{0.1}$	0.1 M KOH	0.255	69	1.592	0.362	This work
$BCF(ZY)_{0.1}$	**1 M KOH**	**0.255**	**66**	**1.554**	**0.324**	**This work**
$Ba_{0.5}Sr_{0.5}Co_{0.8}Fe_{0.2}O_{3-\delta}$	0.1 M KOH	0.255	80	1.612	0.382	This work
IrO_2	0.1 M KOH	0.255	73	1.624	0.394	This work
$Ba_{0.5}Sr_{0.5}Co_{0.8}Fe_{0.2}O_{3-\delta}$	0.1 M KOH	0.32	84	1.72	0.49	*ACS Appl. Mat. Interfaces* 2015, 7, 17663
$Ba_{0.5}Sr_{0.5}Co_{0.8}Fe_{0.2}O_{3-\delta}$	0.1 M KOH	0.232	94	1.74	0.51	*Angew. Chem. Int. Ed.* 2015, 54, 3897
$SrSc_{0.025}Nb_{0.025}Co_{0.95}O_{3-\delta}$	0.1 M KOH	0.36	-	1.63	0.40	*Mater. Horiz. 2015, 2,495*
80 nm $LaCoO_3$	0.1 M KOH	0.25	69	1.72	0.49	*Nat. Commun.*2016, 7,11510
$CaCu_3Fe_4O_{12}$	0.1 M KOH	0.25	51	1.615	0.385	*Nat. Commun.*2015, 6, 8249
$BaCo_{0.7}Fe_{0.2}Sn_{0.1}O_{3-\delta}$	0.1 M KOH	0.232	69	1.655	0.425	*Adv. Sic.* 2016, 3, 1500187
$SrNb_{0.1}Co_{0.7}Fe_{0.2}O_{3-\delta}$	0.1 M KOH	0.232	76	1.73	0.5	*Angew. Chem. Int. Ed.* 2015, 54, 3897

Ball milled $SrNb_{0.1}Co_{0.7}Fe_{0.2}O_{3-\delta}$	0.1 M KOH	0.232	90	1.649	0.419	*Angew. Chem. Int. Ed.* 2015, 54, 3897
$SrNb_{0.1}Co_{0.7}Fe_{0.2}O_{3-\delta}$- *nano-rod*	0.1 M KOH	0.232	61	1.62	0.389	*Adv, Energy Mater.* 2017, 7,1602122
$SrNb_{0.1}Co_{0.7}Fe_{0.2}O_{3-\delta}$- *nano-rod*	1 M KOH	0.232	48	1.62	0.370	*Adv, Energy Mater.* 2017, 7,1602122
$Ba_{0.5}Sr_{0.5}Co_{0.8}Fe_{0.2}O_{3-\delta}$ Solid-state reaction	0.1 M KOH	0.232	80	1.625	0.395	*Electrochim. Acta* 2016, 219, 553
$PrBa_{0.5}Sr_{0.5}Co_{1.5}Fe_{0.5}O_{5+\delta}$ (nanofiber 20nm diameter)	0.1 M KOH	0.202	52	1.58	0.35	*Nat. Commun.*2017, 8,14586
$PrBa_{0.5}Sr_{0.5}Co_{1.5}Fe_{0.5}O_{5+\delta}$ (nanofiber 83nm diameter)	0.1 M KOH	0.202	55	1.61	0.38	*Nat. Commun.*2017, 8,14586
$PrBa_{0.5}Sr_{0.5}Co_{1.5}Fe_{0.5}O_{5+\delta}$	0.1 M KOH	0.202	67	1.716	0.486	*Nat. Commun.*2017, 8,14586
$SrCo_{0.95}P_{0.05}O_{3-\delta}$	0.1 M KOH	0.232	84	1.7113	0.4813	*Adv. Funct. Mater.* 2016, 26,5862
$La_{0.9}FeO_{3-\delta}$	0.1 M KOH	0.232	54	1.64	0.41	*Chem. Mater.* 2016, 28,1691
50 nm $La_{0.7}(Ba_{0.5}Sr_{0.5})_{0.3}Co_{0.8}Fe_{0.2}O_{3-\delta}$	0.1 M KOH	0.64	97	1.60	0.37	*Energy Environ. Sci.* 2016, 9, 176
BSCF treated at 950 °C under O_2 for 48 h	0.1 M KOH	0.64	129	1.78	0.55	*Adv. Mater.* 2015, 27,266
$Ba_{0.5}Sr_{0.5}Co_{0.8}Fe_{0.2}O_{3-\delta}$	0.1 M KOH	0.639	99	1.75	0.52	*Adv. Energy Mater.* 2015, 5, 1501560
IrO_2	0.1 M KOH	0.202	59	1.624	0.394	*Nat. Commun.*2017, 8,14586

IrO_2	0.1 M KOH	0.232	83	1.678	0.448	*Angew. Chem. Int. Ed.* 2015, 54, 3897
IrO_2	0.1 M KOH	0.639	>99	> 1.8	> 0.57	*Adv. Energy Mater.* 2015, 5, 1501560
Co/CoP-HNC	1 M KOH	1	-	1.68	0.45	*Mater.Horiz., 2018, 5,108*
CoMnP nanoparticles	1 M KOH	0.28	95	1.56	0.33	*J. Am. Chem. Soc. 2016, 138, 4006*
CoP nanorods/C	1 M KOH	0.71	-	1.57	0.34	*Energy Environ. Sci. 2015, 51, 11626*
CoP nanoparticles/C	1 M KOH	0.71	-	1.57	0.34	*Energy Environ. Sci. 2015, 51, 11626*

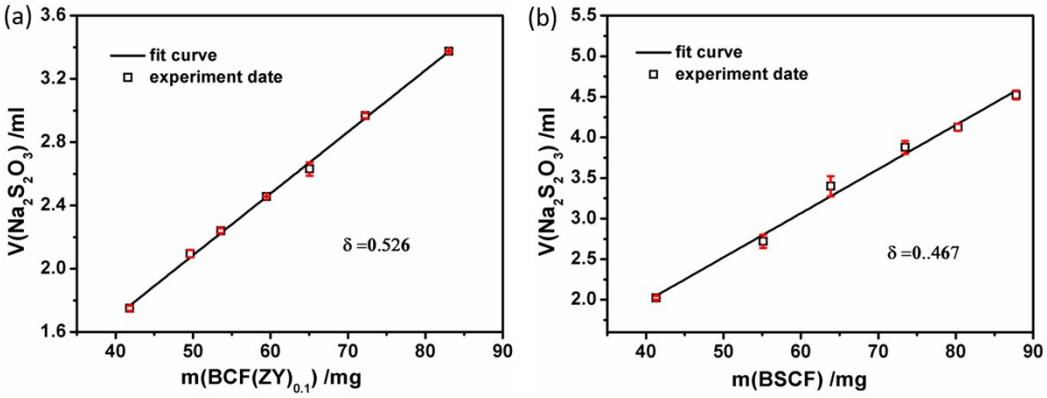

Figure S12. The oxygen vacancy concentration δ of $BCF(ZY)_{0.1}$ and BSCF obtained reliably through parallel iodometric experiment dates with good linear relation.

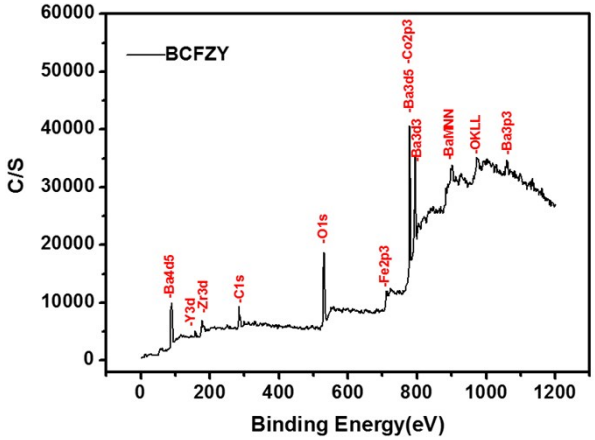

Figure S13. Low resolution XPS spectra of $BCF(ZY)_{0.1}$ collected at room temperature.

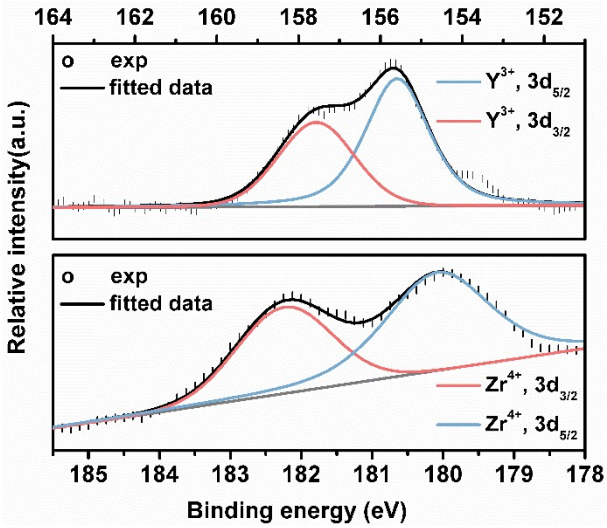

Figure S14. High resolution XPS spectra of Y 3d and Zr 3d core levels of $BCF(ZY)_{0.1}$.

Table S3. Percentage contribution of the four oxygen species of $BCF(ZY)_{0.075}$, $BCF(ZY)_{0.1}$ and BSCF from the deconvoluted results of O 1s XPS spectra.

	O Ⅰ (O^{2-})	O Ⅱ (O_2^{2-}/O^-)	O Ⅲ (O_2)	O Ⅳ (molecular water adsorbed on the surface)
$BCF(ZY)_{0.1}$	26.92%	28.25%	40.77%	4.05%
$BCF(ZY)_{0.075}$	28.59%	23.78%	35.43%	12.20%
BSCF	6.85%	21.15%	52.19%	19.81%

O 1s XPS spectra can be deconvoluted into four different characteristic peaks, i.e., lattice oxygen species (~528.96 eV for O^{2-}), reactive oxygen species (~530.67 eV for O_2^{2-}/O^-), the surface adsorbed oxygen (~531.46 eV for O_2), and adsorbed molecular water or carbonates (~ 532.87 eV for H_2O).

Table S4. The ratios of Co^{3+} (3 d^6) / Co^{2+} (3 d^7) and Fe^{3+} (3 d^5) / Fe^{2+} (3 d^6) in $BCF(ZY)_{0.1}$ calculated as per the respective area intensity of characteristic peaks from the deconvoluted results of high resolution XPS spectra.

	Co^{2+}	Co^{3+}	Fe^{2+}	Fe^{3+}
Percentage (of the Co/Fe in BCFZY)	15.41%	84.59%	25.35%	74.65%

Table S5. Fitted Mössbauer parameters of $BCF(ZY)_{0.1}$.

spectrum	Isomer shift (mm/s)	Quadrupole splitting (mm/s)	FWHM (mm/s)	Area Ratio (%)
Doublet 1	0.49(1)	0.82(1)	0.33(3)	25.3
Doublet2	0.214(9)	0.859(6)	0.49(2)	74.7

Table S6. Bader charges analysis of fully oxidized and relaxed structure with a large cell $Ba_{20}Co_8Fe_8Zr_2Y_2O_{60}$. (here, q=valence electrons-charge (valence electrons: 6 for O, 8 for Fe, 9 for Co, 11 for Y, 12 for Zr and 10 for Ba)).

	X	Y	Z	Charge	Atom Charge (q)	Avg. charge transfer
O1	7.878564	1.994766	2.013621	7.044751	-1.044751	-1.065035828
O2	1.988081	0.221619	1.972395	7.002184	-1.0021843	
O3	1.988081	1.994766	20.11325	7.0041	-1.0041003	
O4	4.049919	1.994766	2.013621	7.044751	-1.044751	
O5	5.964242	0.098286	1.994666	7.175648	-1.175648	
O6	5.964242	1.994766	0.100234	7.135085	-1.1350851	
O7	0.107587	5.984298	1.941141	7.210255	-1.2102545	
O8	1.988081	3.767914	1.972395	7.002184	-1.0021843	
O9	1.988081	5.984298	0.096391	7.038965	-1.0389645	
O10	3.868574	5.984298	1.941141	7.210255	-1.2102545	
O11	5.964242	3.891246	1.994666	7.175648	-1.175648	
O12	5.964242	5.984298	20.05527	7.184543	-1.1845425	
O13	7.868576	1.994766	6.140591	7.00263	-1.0026296	
O14	1.988081	0.066857	6.158777	7.060328	-1.0603278	
O15	1.988081	1.994766	4.342387	6.994706	-0.9947059	
O16	4.059907	1.994766	6.140591	7.00263	-1.0026296	
O17	5.964242	0.185426	6.119492	7.094637	-1.0946366	
O18	5.964242	1.994766	4.00855	6.97746	-0.9774602	
O19	0.22793	5.984298	6.113889	7.125415	-1.1254148	
O20	1.988081	3.922675	6.158777	7.060328	-1.0603278	
O21	1.988081	5.984298	3.754759	6.999855	-0.999855	
O22	3.748232	5.984298	6.113889	7.125415	-1.1254148	
O23	5.964242	3.804107	6.119492	7.094637	-1.0946366	
O24	5.964242	5.984298	3.964431	7.326304	-1.3263035	
O25	7.891956	1.994766	10.22205	7.19201	-1.1920104	
O26	1.988081	7.887297	10.18226	7.204938	-1.2049381	
O27	1.988081	1.994766	8.082298	7.153632	-1.1536323	
O28	4.036527	1.994766	10.22205	7.19201	-1.1920104	
O29	5.964242	7.823345	10.23408	6.95415	-0.9541503	
O30	5.964242	1.994766	8.507084	6.94663	-0.9466303	
O31	0.04167	5.984298	10.18003	6.966976	-0.9669758	
O32	1.988081	4.081299	10.18226	7.204938	-1.2049381	
O33	1.988081	5.984298	8.254608	6.969285	-0.9692851	
O34	3.934491	5.984298	10.18003	6.966976	-0.9669758	
O35	5.964242	4.145251	10.23408	6.95415	-0.9541503	
O36	5.964242	5.984298	8.33439	7.147114	-1.147114	
O37	7.88596	1.994766	14.128	6.987626	-0.987626	
O38	1.988081	7.891111	14.15783	7.046092	-1.0460918	
O39	1.988081	1.994766	12.3038	7.152569	-1.1525687	
O40	4.042523	1.994766	14.128	6.987626	-0.987626	

O41	5.964242	0.085544	14.12959	7.063242	-1.0632418	
O42	5.964242	1.994766	12.08771	6.998138	-0.998138	
O43	0.017257	5.984298	14.1582	7.034304	-1.0343044	
O44	1.988081	4.077485	14.15783	7.046092	-1.0460918	
O45	1.988081	5.984298	12.08955	6.955697	-0.955697	
O46	3.958905	5.984298	14.1582	7.034304	-1.0343044	
O47	5.964242	3.903989	14.12959	7.063242	-1.0632418	
O48	5.964242	5.984298	12.20696	7.045377	-1.0453774	
O49	0.188478	1.994766	18.09876	7.101422	-1.1014221	
O50	1.988081	7.902992	18.13119	7.035518	-1.0355175	
O51	1.988081	1.994766	16.07092	6.99681	-0.9968098	
O52	3.787683	1.994766	18.09876	7.101422	-1.1014221	
O53	5.964242	7.7887	18.12265	7.066652	-1.0666524	
O54	5.964242	1.994766	15.97004	7.090721	-1.0907211	
O55	0.097313	5.984298	18.14636	7.016247	-1.0162467	
O56	1.988081	4.065604	18.13119	7.035518	-1.0355175	
O57	1.988081	5.984298	16.16443	6.970914	-0.9709136	
O58	3.878848	5.984298	18.14636	7.016247	-1.0162467	
O59	5.964242	4.179897	18.12265	7.066652	-1.0666524	
O60	5.964242	5.984298	16.1174	7.044198	-1.0441976	
Fe1	5.964242	1.994766	1.954128	6.310792	1.6892085	1.53738875
Fe2	1.988081	5.984298	1.955605	6.435247	1.5647531	
Fe3	1.988081	1.994766	6.144414	6.42862	1.5713805	
Fe4	5.964242	1.994766	5.903226	6.545956	1.454044	
Fe5	1.988081	5.984298	10.2112	6.539769	1.4602308	
Fe6	5.964242	5.984298	10.20896	6.49447	1.50553	
Fe7	5.964242	1.994766	14.16327	6.469455	1.5305453	
Fe8	1.988081	5.984298	18.01226	6.476582	1.5234178	
Co1	1.988081	1.994766	1.792863	7.660261	1.339739	1.37668935
Co2	1.988081	5.984298	6.320506	7.617704	1.3822958	
Co3	5.964242	1.994766	10.25959	7.577019	1.4229807	
Co4	1.988081	1.994766	14.18298	7.607932	1.3920678	
Co5	1.988081	5.984298	14.12446	7.648983	1.3510174	
Co6	5.964242	5.984298	14.16714	7.648455	1.3515453	
Co7	1.988081	1.994766	18.05023	7.647577	1.3524231	
Co8	5.964242	5.984298	18.09868	7.578554	1.4214457	
Y1	5.964242	5.984298	6.117712	8.888231	2.1117694	2.0746143
Y2	5.964242	1.994766	18.14771	8.962541	2.0374592	
Zr1	5.964242	5.984298	1.931896	9.508315	2.491685	2.4617265
Zr2	1.988081	1.994766	10.21167	9.568232	2.431768	
Ba1	0.071253	7.96534	20.13332	8.427996	1.5720039	1.57584484
Ba2	3.904908	7.96534	20.13332	8.427996	1.5720039	
Ba3	0.071253	4.003256	20.13332	8.427996	1.5720039	
Ba4	3.904908	4.003256	20.13332	8.427996	1.5720039	
Ba5	0.079245	0.054306	4.039946	8.425254	1.5747458	
Ba6	3.896916	0.054306	4.039946	8.425254	1.5747458	
Ba7	0.079245	3.935227	4.039946	8.425254	1.5747458	
Ba8	3.896916	3.935227	4.039946	8.425254	1.5747458	
Ba9	7.936489	0.020187	8.184677	8.426642	1.5733585	
Ba10	3.991994	0.020187	8.184677	8.426642	1.5733585	

Ba11	7.936489	3.969345	8.184677	8.426642	1.5733585
Ba12	3.991994	3.969345	8.184677	8.426642	1.5733585
Ba13	7.929722	7.93869	12.20712	8.416095	1.5839048
Ba14	3.998762	7.93869	12.20712	8.416095	1.5839048
Ba15	7.929722	4.029906	12.20712	8.416095	1.5839048
Ba16	3.998762	4.029906	12.20712	8.416095	1.5839048
Ba17	0.023682	7.94094	16.09157	8.424789	1.5752112
Ba18	3.952479	7.94094	16.09157	8.424789	1.5752112
Ba19	0.023682	4.027656	16.09157	8.424789	1.5752112
Ba20	3.952479	4.027656	16.09157	8.424789	1.5752112

NUMBER OF ELECTRONS: 741.9999
SUM OF THE ATOMS CHARGE: 5.35E-05

[1] J. P. Perdew, K. Burke, M. Ernzerhof, *Physical Review Letters* 1997, 78, 1396.
[2] G. Kresse, J. Furthmuller, *Computational Materials Science* 1996, 6, 15.
[3] G. Kresse, D. Joubert, *Physical Review B* 1999, 59, 1758.
[4] P. E. Blochl, *Physical Review B* 1994, 50, 17953.
[5] M. R. Li, M. W. Zhao, F. Li, W. Zhou, V. K. Peterson, X. Y. Xu, Z. P. Shao, I. Gentle, Z. H. Zhu, *Nature Communications* 2017, 8.